coatings

MDPI

Article

Effective Detection of the Machinability of Stainless Steel from the Aspect of the Roughness of the Machined Surface

Miroslav Duspara [1], Borislav Savković [2,*], Branislav Dudic [3,4,*] and Antun Stoić [1]

[1] Mechanical Engineering Faculty in Slavonski Brod, University of Slavonski Brod, 35000 Slavonski Brod, Croatia
[2] Faculty of Technical Sciences, University of Novi Sad, 21000 Novi Sad, Serbia
[3] Faculty of Management, Comenius University Bratislava, 81499 Bratislava, Slovakia
[4] Faculty of Economics and Engineering Management, University Business Academy, 21000 Novi Sad, Serbia
* Correspondence: savkovic@uns.ac.rs (B.S.); branislav.dudic@fm.uniba.sk (B.D.)

Abstract: Reliable measurement of surface roughness (Ra) is extremely important for quality control of production processes. The cost of the equipment and the duration of the measurement process are very high. The aim of this work is to develop a device for non-destructive measurement of specific roughness levels on stainless steel using computer vision. The device should be structurally simple, affordable, accurate, and safe for practical use. The purpose of the device is to effectively detect the level of roughness of the treated surface obtained by the water jet cutting process. On the basis of the obtained results, it is possible to adjust the parameters during the cutting process. The principle of operation of the device is based on measuring the intensity of the visible spectrum of the light reflected from the surface of the sample to be measured and correlating these values with the values of the measured roughness. After testing several variants of the device, the so-called vertical measurement variant was developed using the following equipment: violet light LED, optical filter and light splitter, USB 2.0 web camera, Arduino microcontroller, personal computer, and LabView programming interface.

Keywords: computer vision; optical measurement; reflection; stainless steel; surface roughness

Citation: Duspara, M.; Savković, B.; Dudic, B.; Stoić, A. Effective Detection of the Machinability of Stainless Steel from the Aspect of the Roughness of the Machined Surface. *Coatings* **2023**, *13*, 447. https://doi.org/10.3390/coatings13020447

Academic Editor: Tadeusz Hryniewicz

Received: 21 January 2023
Revised: 13 February 2023
Accepted: 13 February 2023
Published: 16 February 2023

1. Introduction

Control of surface quality is becoming increasingly important, especially in the production of precise elementary parts [1]. The task of production is to create surfaces that provide satisfactory machinability at minimum cost. The control of surface quality includes the determination of micro- and macro-geometric characteristics, i.e., roughness of the treated surface [2,3]. The criterion for determining the degree of roughness for a particular type of machining is given by the corresponding standard.

Machining quality is determined by two fundamentally similar meanings. The first meaning is that the quality refers to the machined surface obtained by removing material using various machining processes, such as laser machining [4,5], milling [6,7], drilling [8], or some other advanced processes [9]. Another meaning is that quality refers to the work and represents a set of indicators that determine its value and utility. The manufactured part consists of several machined surfaces, each of which can be manufactured using different technology. The geometry of the machined surface results from a combination of three elements:

Surface roughness, which refers to high-frequency irregularities on the treated surface [10]. It is caused by displacement marks, reflections of the profile of the tool tip, traces of abrasive particles, etc.

Surface waviness, which represents medium-frequency irregularities on the treated surface [11].

Surface shape, which represents the general shape of the surface if roughness and waviness are ignored [12].

In addition, the physical and mechanical properties of the surface layers after processing are determined by consolidation, depth of consolidation, distribution and degree of consolidation, structure of the consolidation layer, and residual stresses. The concept of surface integrity, originally defined for grinding operations, can be extended to other finishing operations and includes six different groups of key factors: visual, dimensional, residual stress, tribological, metallurgical, and other factors [13–16]. It should be noted that all parameters in the material removal process have a direct impact on the integrity of the machined workpiece surface [13,17,18].

Today, process-independent and in-process measurement systems are used to measure the roughness parameters of the machined surface [19]. When using out-of-process measurement systems for roughness measurement, the cutting process must be interrupted at the desired time, and then the value of the roughness parameter must be measured. Process sensors can be classified according to various criteria: direct or indirect, contact or non-contact, and intermittent or continuous [20]. Various principles can be used for measurement: mechanical, optical, electrical, pneumatic, etc. Accordingly, the types of sensors for measuring the roughness of the treated surface can be mechanical, optical, electromagnetic, capacitive, piezoelectric, frequency, electromechanical, or a combination. The problems faced by researchers on this subject are varied. Thus, we find systems that perform roughness measurements with an insufficient measurement range, i.e., with a narrow range of the obtained data [21,22]. Moreover, the inaccessibility of the measurement poses a very large problem. Such a problem occurred, for example, when measuring the roughness of the wheels of moving trains, which produced loud acoustic noises the source of which had to be determined [23]. Generally, various approaches to this issue were explored, but due to their precision and measurement range, i.e., expensive instrumentation, they encountered difficulties [24].

The most commonly used method to evaluate the texture of the treated surface is a probe that is mechanically passed over the surface. The field of surface evaluation techniques is continually developing, and non-contact methods are most commonly used for on-line evaluation of the treated surface [25,26]. Again, the optical probes used vary. Depending on chromatic confocality, they can be intended for transparent or non-breathable materials [27,28].

Laser triangulation is one of the simplest non-contact measurement methods. It is based on the fact that the degree of reflection from the processed surface depends on its roughness [29].

In various machining processes based on material removal, specific qualities of the machined surface are obtained. Accordingly, a distinction is made between fine machining processes, such as grinding or scraping, again focusing on the creation of appropriate models of the output characteristics of the process, in this case, surface roughness. These models can be mathematical, i.e., based on artificial intelligence [30,31]. In addition to these precise technologies of cutting processing, some processing where such low roughness is not achieved finds its share of attention. These certainly include machining with an abrasive water jet, which is most commonly used when working with difficult-to-machine materials where thermal treatment of the surface should be avoided [32,33]. The challenge is to obtain, in the most economical and productive way, information about the quality of machining from the aspect of roughness. This is certainly achieved through the formation of appropriate models of the behavior of the treated surface as a function of variable parameters, on the basis of which appropriate optimization of the process is carried out [34,35].

One of the most common problems in measuring the roughness of surfaces is that a classical device with a measuring probe cannot reach the surface on which the level of roughness needs to be determined. Problems arise due to the overall dimensions of the device with the tentacle, as well as various films that hinder the movement of the tentacle.

The device presented later in this paper provides a quick and effective way to determine the level of surface quality. The disadvantage of the previously mentioned measurement variants is the installation cost itself, which is several times higher than the device proposed in this paper. The paper presents the approach of surface measurement after water jet treatment on an austenitic steel. However, the application range of the device is wide. Accordingly, it is possible to perform measurements on a variety of materials; for example, to determine whether they are metallic, non-metallic or, wooden [36], it is only necessary that a certain degree of reflection is observed.

It should also be noted that the daily development of appropriate coatings, i.e., films used to treat surfaces after machining, affects the change in roughness, i.e., the quality of the surface [37]. Accordingly, this device can quickly detect the influence of certain coatings that have been used on the surface, as well as various thermal treatments [38].

The general purpose and goal of this research is to create a new prototype device that will quickly and efficiently contribute to the detection of the quality of the treated surface from the aspect of roughness. In addition, the authors would like to show that it is possible, even with very modest resources, to develop an adequate device for the rapid detection of surface roughness. Here, the emphasis is primarily on non-contact measurement of inaccessible surfaces.

The novelty of the research is a device that works on the principle of optical reflection of light, where the detected image is measured in bits as a unit to define the image quality of the corresponding surface. The bits defined in this way are indirectly translated into a size that defines the roughness of the machined surface, which is micrometers.

2. Experimental Setup

The paper describes an optical method for measuring the roughness of the treated surface on samples that were cut with a high-pressure water jet. After cutting the samples, the roughness of the treated surface was measured using a Mitutoyo SJ301 (Kanagawa, Japan) device (Figure 1).

Figure 1. Surface roughness measurement with portable tester Mitutoyo SJ 301 SurfTest.

The measured roughness was compared with the light scattering of an optical roughness meter. These are determined classes of light intensity with regard to the roughness of the treated surface.

Figure 2a shows the principle of light reflection from smooth surfaces, where reflection occurs at the same angle of incidence. In the case of a rough surface (Figure 2b), the light is scattered at other angles.

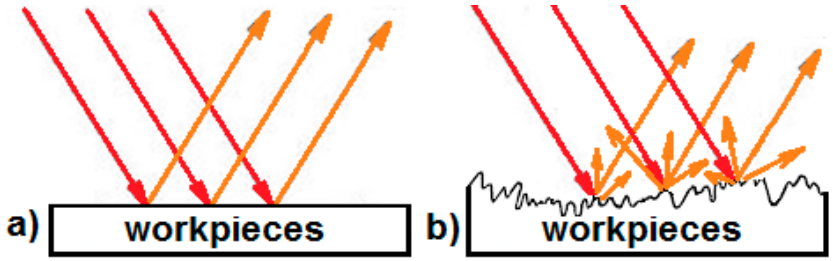

Figure 2. Light reflection: (**a**) smooth surface and (**b**) rough surface.

In order to avoid the problems caused by the variable distance as well as by the construction design, a vertical orientation was applied. In addition, when the light is collimated, there is no need to fix the exact distance from the observed sample. This design of the device offers the possibility to divide the light beam with the help of a splitter. This uniform division of the light beam in the amount of 50% is possible if the splitter is placed at an angle of 45° in relation to the horizontal. In this case, half of the light is transmitted to the sample, while the other half is reflected. The amount of this reflected light is 25% less than the light source, since the sample cannot be considered to act as an ideal mirror. The reception of this light is accomplished by an optical sensor located on the side. This type of design is the most expensive and also the most effective. In experimental measurements, the distance of the device does not affect the amount of light detected by the sensor because the influence of the angle of incidence is avoided in a vertical orientation. It should also be taken into account that the light source is extremely bright because the light beam must pass through the splitter twice. If this is not ensured, there is a possibility of a loss of light intensity of 75% (Figure 3).

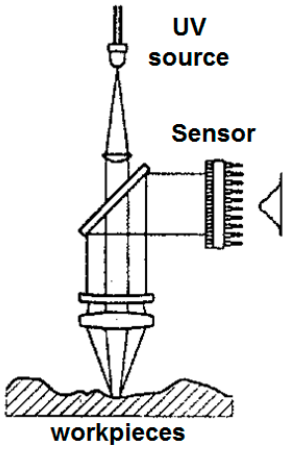

Figure 3. Vertical orientation of optical measurement.

2.1. Construction of the Device

During the construction of the housing for accepting the device, it is necessary to ensure sufficient distance between the device and the sample to further implement it through the assembly line. The housing of the device was designed in Solidworks and then fabricated from acrylonitrile butadiene styrene (ABS) using a 3D printer. Figure 4 shows the two main parts. The larger part is intended for the Arduino microcontroller, the signal lamp, and the beam splitter. The smaller part serves to hold the USB camera. In addition, it is necessary to have the LabVIEW software installed on the computer and to be connected to the web camera.

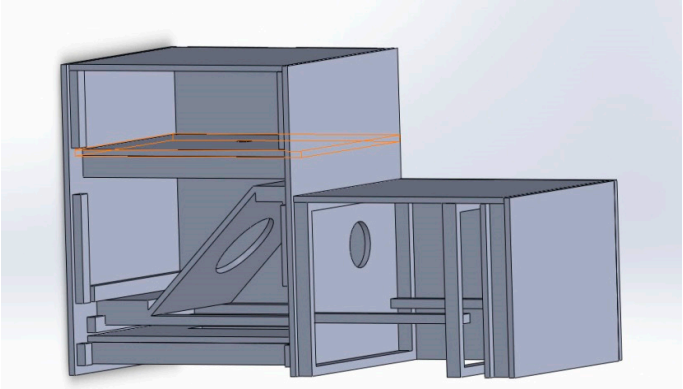

Figure 4. Prototype design of a box fabricated on a 3D printer, with a lens holder at an angle of 45°.

2.2. System Main Elements

2.2.1. Light Source, Lens, and USB Camera

Regarding the light source, we must emphasize both the magnitude of the intensity and the type of wavelength. The wavelength has a great effect in terms of accuracy or resolution, as well as the safety of the device itself. It is important to note that some wavelengths are harmful and can have undesirable effects, such as ultraviolet light. The following equipment was used:

Purple LED (SSL-LX5093VC), Lumex Opto/Components Inc (Carol Stream, IL, USA): This source produces 2200 mcd and λ = 550 nm at an operating current of 20 mA (Figure 5a).

Figure 5. (**a**) Led SSL-LX5093VC, (**b**) Thorlabs beam splitter EBS1, and (**c**) USB camera.

The Thorlabs (Newton, NJ, USA) EBS1 50:50 (at 45° angle of incidence) beam splitter: operating in the visible (450–600 nm) spectrum (Figure 5b).

USB digital microscope KLN-J200 (Kalinu Technology CO., LTD, Ningbo, China): 2.0 Mpx, usb 2.0, zoom 25×–200×, focus manual (0–85 mm), image resolution from 320 × 240 to 1600 × 1200, video resolution 640 × 480 (Figure 5c).

The lens is semi-conducting and must be positioned at a precise 45° angle, as the reflected light must fall on the camera as much as possible.

The difference between the presented device and the existing ones is that it uses a fast optical measurement of light reflection from the surface compared with mechanical (measuring probe). In addition, compared with optical measuring devices, the developed device uses a wavelength of 550 nm LED.

2.2.2. The Procedure of Image Detection and Analysis

A combination of multiplication methods was used for image analysis, i.e., defining classes for the roughness value Ra. The flowchart shows that the algorithm first captures the image, then converts the raw image into gray scale, defining the appropriate level of values in terms of light intensity. After that, an area predefined by the user within the image is viewed; this is the ROI (region of interest), which can be a square area or a line, and its appropriate type is selcted by the user on the basis of the application interface. The intensity values within this area are then averaged, and that average intensity is then correlated to a specific class of Ra, defined by the numerous measurements of test samples

with known values of surface roughness for device calibration. If the light intensity is outside the defined classes, the algorithm indicates an error, i.e., an unknown value of the roughness parameter. This is shown in the flowchart in Figure 6.

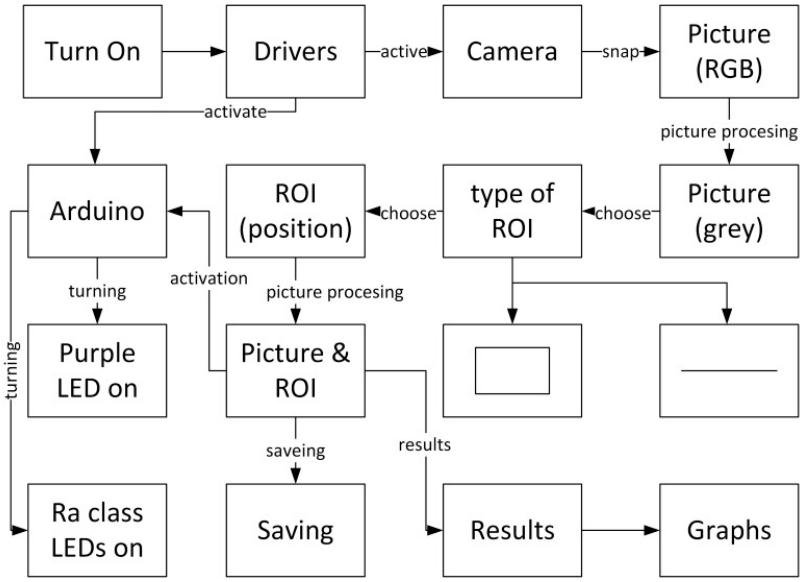

Figure 6. Application flowchart.

The mathematical algorithm itself is not defined, and the principle of operation of this device is to control the hardware units, in this case, the LED lamp, through software. For the realization of this control, the software package LabView is used, which operates on the principle of graphical programming and uses various icons and connectors on the basis of which the front panel, i.e., the virtual device, is defined. The front panel obtained in this way essentially simulates an instrument. Further connection of the injector units is carried out through the block diagram, which is an integral part of this device.

2.3. Application User Interface (UI)

The interface is adapted to the user, who can very easily perform measurements (Figure 7). The measurement is performed in several steps. The first step is to place the device directly above the surface of which the roughness is to be measured. Once the positioning is completed, the indicator marked "ON" is pressed in order to start the light source. Then, the indicator labeled "Snap" will be used on the virtual instrument and a recording is captured. When recording, it is necessary to select the ROI (type and position), which is defined in green in the third window. On the user interface, there is also a window called "Live Image", which allows the user to see a potential image before capturing the recording. At the very end, the "Process" button is activated, and the image is processed, that is, the detected value of Ra is determined and displayed.

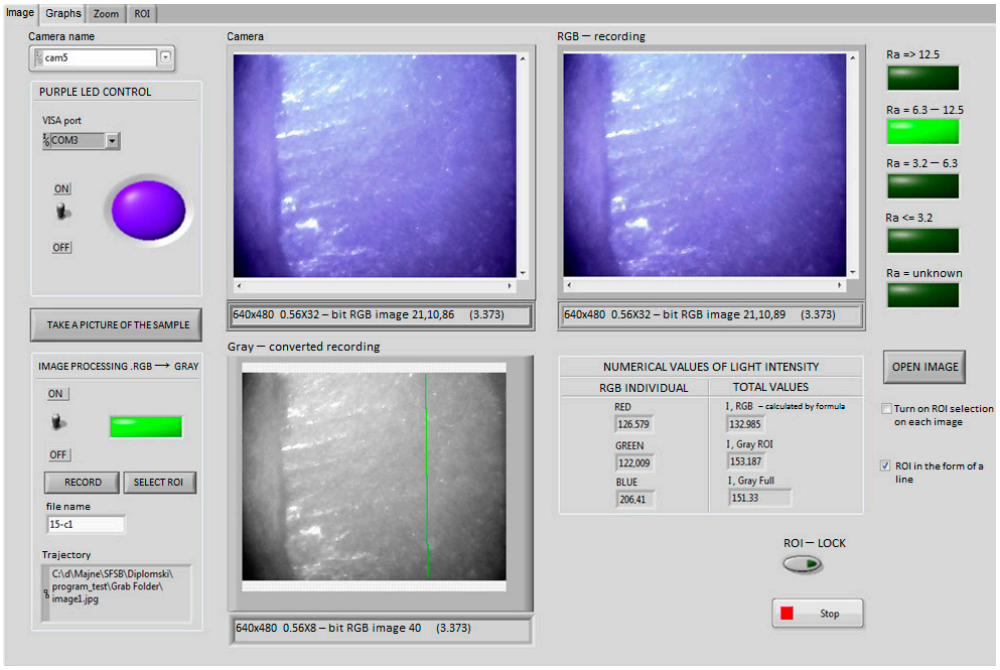

Figure 7. User interface.

After obtaining the Ra class results, the user can see the graphical results on the "Graph" tab and save all the results (image (RGB and gray), intensity value, and graph) by pressing the "Save" button on the main "Image" tab (Figure 8).

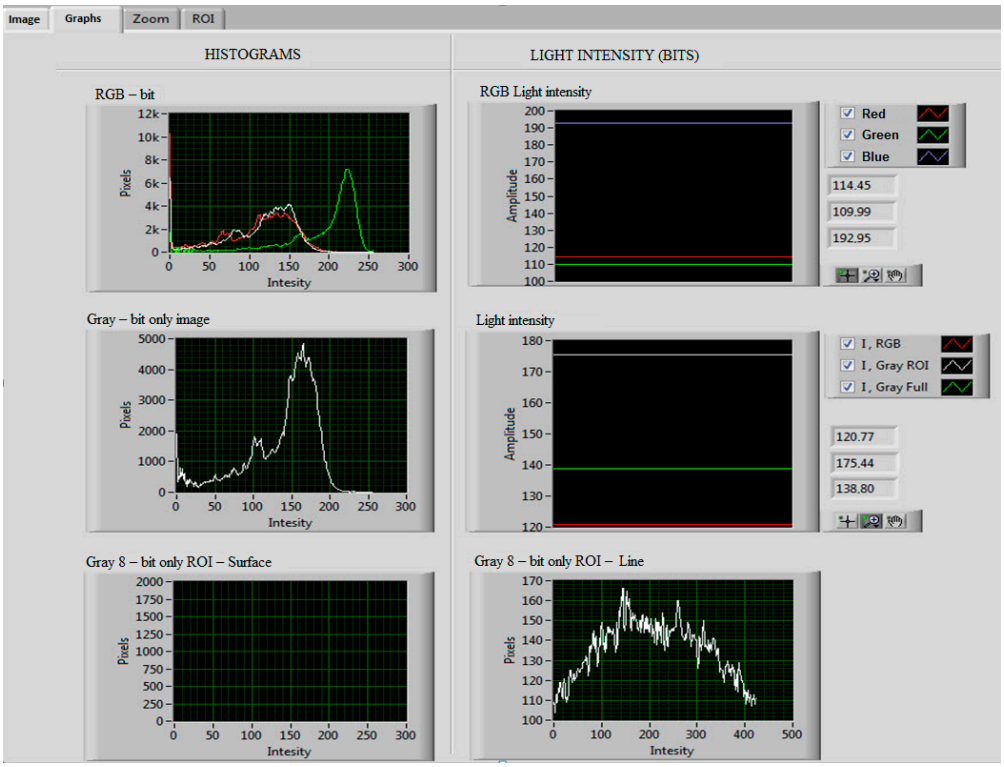

Figure 8. Graph results in the "Graph" tab.

3. Results of Measurements

The machine used was Teen King 1530 (Foshan City, Guangdong, China), dimensions of the work table 3000 × 1500, the cutting speed was 22–35 mm/min, the water pressure

was 3000–3500 bar, and the mass flow of Barton Garnet abrasive was 0.32–0.5 kg/min. These parameters were varied during the experiment and are the most important for the cutting quality, the cutting speed being the most influential parameter.

The corrosion-resistant austenitic steel (AISI 316L) was used as the machining material (Table 1). The large thickness (30 mm) of the plate affected the efficiency of cutting, and accordingly, the structure of the water jet was modified by adding abrasive material particles (Barton Garnet Mesh No. 80).

Table 1. Sample measurement results.

Sample No.	Measured Ra, μm	Measurements with a Camera C1 (Bits)							Mean Value
		M1	M2	M3	M4	M5	M6	M7	
1	3.74	158.15	161.88	156.74	162.18	155.86	161.67	161.15	159.66
1a	3.71	170.31	178.35	167.81	168.85	160.24	180.96	171.41	171.13
2	5.23	159.41	158.79	156.66	156.76	155.16	161.90	161.78	158.64
2a	4.64	166.54	163.36	164.41	167.81	168.08	167.89	164.71	166.11
3	4.41	168.23	166.37	166.41	169.77	162.47	161.66	168.09	166.14
3a	5.25	161.39	162.02	163.78	157.72	162.25	156.41	163.25	160.97
4	7.07	149.50	150.34	154.91	154.08	146.78	143.05	150.52	149.88
4a	5.82	162.36	161.49	159.91	160.59	159.09	162.69	159.00	160.73
5	5.83	172.71	172.12	171.62	165.56	173.88	174.15	176.50	172.36
5a	6.12	165.32	163.09	168.17	161.01	164.87	169.62	169.81	165.98
6	5.61	166.28	172.80	166.66	170.01	165.86	163.60	163.26	166.92
6a	4.95	173.99	175.44	169.10	178.27	170.32	171.61	170.24	172.71
7	6.42	149.11	145.29	151.28	150.14	154.73	152.07	147.45	150.01
7a	5.37	165.07	161.76	166.23	162.69	169.22	169.02	164.87	165.55
8	13.52	137.28	141.38	144.45	135.12	139.78	144.89	140.04	140.42
8a	16.03	135.91	137.42	127.80	139.34	143.22	142.17	139.48	137.91

Table 1 shows the results of measurements with the Mitutoyo SJ 301 SurfTest device (Ra, μm), as well as measurements with cameras (*C*1, bits). The roughness values for one interval were measured twice, where the repeated measurement is represented by the prefix "a". The values from M1 to M7 are repeated measurements aimed at the same surface, in order to show the measurement error, which is approximately 2%, and was determined on the basis of Equation (1).

$$\Delta = \sum_{i=1}^{n} \frac{\left|C1_i - \overline{C1}\right|}{\overline{C1}} / n \cdot 100\% \quad (1)$$

where *C*1 is each individual measurement,

- $\overline{C1}$ is the mean value of individual (n) measurements,
- $i = 1, 2.3...7$.

Considering the measurement results, the following light intensity values for the following roughness classes were adjusted in the application:

1st class: 145 > I (bits) > 135 for Ra > 12.5 μm,
class: 155 > I (bits) > 145 for Ra: 6.3–12.5 μm,
class: 185 > I (bits) > 155 for Ra: 3.2–6.3 μm,
class: 205 > I (bits) > 185 for Ra < 3.2 μm,
class: I (bits) > 205 or I (bits) < 135, Ra: unknown (error).

The maximum roughness value is defined according to the characteristics of the profilometer, which works on the touch principle, and for which the usual value for the maximum possible measured size is approximately 15 μm. Accordingly, the presented device was tested and resulted in a surface quality of greater than 12.5 μm, which can be considered as very rough machining in mechanical engineering. The detection of even greater irregularities would not be useful because one would then enter the realm of undulations.

A roughness of less than Ra = 3.2 µm can generally not be achieved with water jet processing technology. The AISI 316L steel that was tested has a very high profile thickness; therefore, it is very difficult to achieve such a good quality of the machined surface while still maintaining an economical cutting. It can be assumed that all surfaces that have more than 205 bits would have better reflection and lower roughness.

Some problems that may occur during measurement should also be mentioned. If a layer of water and/or dirt is minimal and is evenly distributed over the entire surface in the form of a film, the measurement results likely would not deviate significantly, i.e., they would remain in the same class of roughness as if the surface were completely clean. However, any non-uniformity and a larger amount of cutting products would certainly affect the reflection band.

In addition, the results will be affected by the material of the surface that is being tested, and it is necessary to determine the level of reflection for each new material. Materials for which this method does not work are those that do not produce surface reflection when illuminated with photons, thus preventing the camera sensor from reading them. These include paper, rubber, leather, glass, etc.

Statistical Analysis of Optical Measured

Data processing was performed in the Statistica program and the Student's distribution was used. Since the number of tested samples was less than 30, this statistical method of data processing is proven to be the most applicable.

From the box and whisker plot, it can be seen that the rougher the processed surface, the greater the intensity of reflected light, i.e., the less light reaches the camera sensor (Figure 9). It is also observed from the mean +/−1 standard deviation that 66% of the data do not overlap with other roughness classes; thus, we can say with a certainty of 66% that this method is sound (Figure 10). Using a better camera (higher resolution) and higher quality optics would produce better and more accurate results.

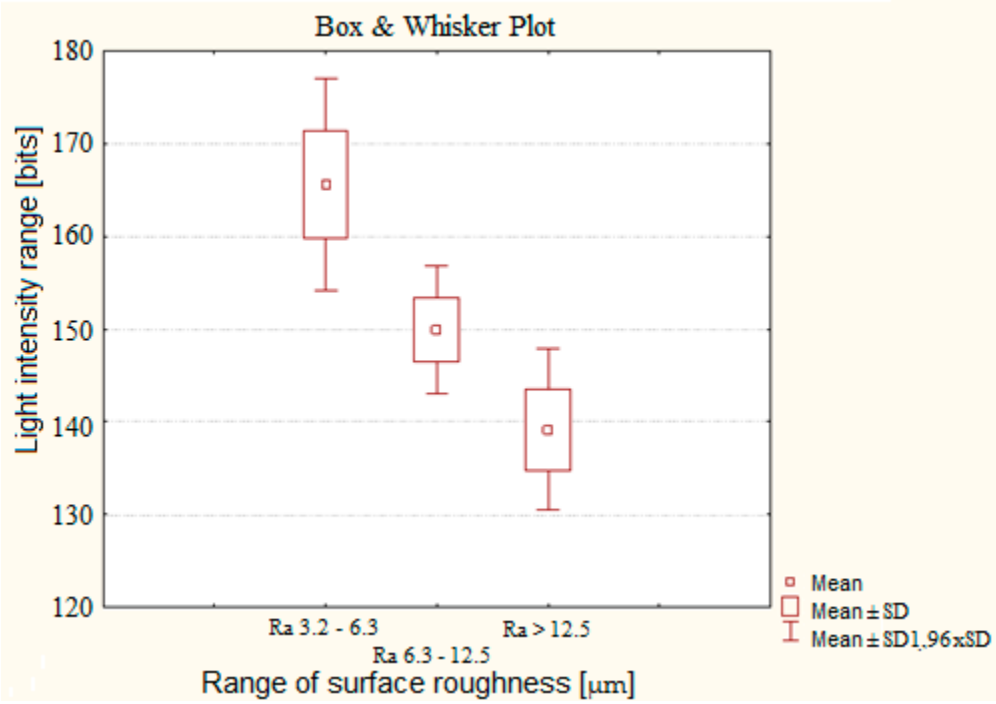

Figure 9. Box-and-whisker plots of the range of light intensity and surface roughness.

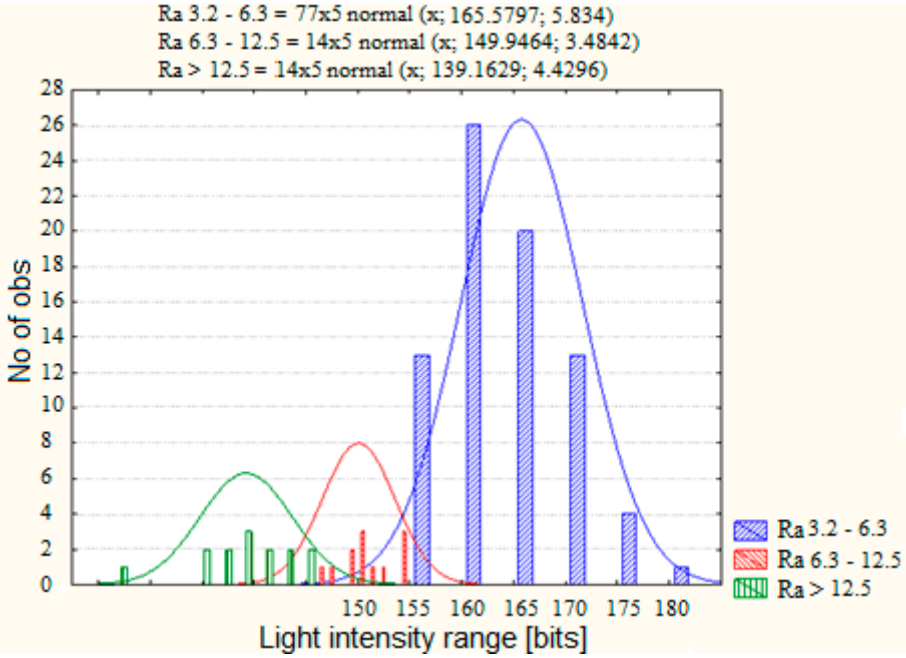

Figure 10. Histograms of multiple variables.

From the graphs, it can be observed from the normal natural Gaussian distribution (center and area of the square) that there is no overlap among the measured data of the surface roughness of the different classes (the square accounts for 66% of the data). For Classes 2 and 3, this discrepancy is obvious, which shows that this method is best for measuring roughness for these classes. There is only some slight overlap in the data at the edges, so we can say that the percentage of accuracy is higher, for these classes. In addition, the distance between Classes 1 and 2 is smaller and there is more overlap at the edges, but with a better camera (higher resolution) the edge overlaps would decrease.

4. Conclusions

After the final tests and measurements of the test samples, the device for determining the degree of roughness using computer vision has shown that it is possible to build a very affordable device (up to EUR 150) that, with the development of software solutions and under certain production conditions, can replace very expensive and sophisticated devices.. For the sake of comparison, the basic model of the device Mitutoyo SJ 301 costs approximately EUR 3000, and the Taylor and Hobson—Surtronic S100 (Leicester, UK), for example, is even more expensive, at approximately EUR 5000.

The computer vision system allows the user to perform checks and measurements in the production facility without disturbing the production process.

The presented measuring device has its advantages, which are reflected primarily in the fact that it does not require a large financial investment, is very easy to use, and does not require any long-term training. It is also possible to perform a quick test immediately after cutting the piece to determine to which class the quality of the cut belongs and to make corrections to the cutting parameters, such as reducing the cutting speed, increasing the pressure, correcting the abrasive flow, etc.

During tests and measurements, the system shows certain deviations in different series of measurements, which are not negligible. It showed the highest precision when measuring samples with a roughness level between 3.2 and 6.3 µm. Difficulties occurred with the sample with roughness greater than 12.6 µm and less than 3.2 µm.

The direction of future improvement of the device is moving towards the installation of a better camera with a better resolution (more than 8 MP), then better optics that would reduce the variations of the light intensity during the measurement, as well as the

application of new measuring templates that would enable a more accurate positioning on the sample. On the basis of this, it would be possible to define a larger number of roughness classes, focusing on lower values and a quality level below N8 (Ra < 3.2 µm).

The presented device should be very interesting in the industrial sector, where its application is expected. For practical application of the system in production, additional tests on a larger number of samples and provision of the necessary improved equipment are required.

Author Contributions: Conceptualization, M.D. and B.S.; methodology, A.S.; software, M.D. and A.S.; validation, B.S., B.D. and A.S.; formal analysis, M.D.; investigation, B.S.; resources, B.D.; writing—original draft preparation, M.D. and B.S.; writing—review and editing, A.S.; visualization, B.D.; supervision, B.D. and A.S. All authors have read and agreed to the published version of the manuscript.

Funding: This research received no external funding.

Institutional Review Board Statement: Not applicable.

Informed Consent Statement: Not applicable.

Data Availability Statement: Not applicable.

Conflicts of Interest: The authors declare no conflict of interest.

References

1. Minoni, U.; Cavalli, F. Surface quality control device for on-line applications. *Measurement* **2008**, *41*, 774–782. [CrossRef]
2. Savkovic, B.; Kovac, P.; Rodic, D.; Strbac, B.; Klancnik, S. Comparison of artificial neural network, fuzzy logic and genetic algorithm for cutting temperature and surface roughness prediction during the face milling process. *Adv. Prod. Eng. Manag.* **2020**, *15*, 137–150. [CrossRef]
3. Savković, B.; Kovač, P.; Stoić, A.; Dudić, B. Optimization of machining parameters using the Taguchi and ANOVA analysis in the face milling of aluminum alloys Al7075. *Tehnički Vjesnik* **2020**, *27*, 1221–1228.
4. Xu, J.; Sun, G.; Zhai, C.; Tian, J.; Nie, X.; Yu, H. Study on the Heat-Affected Zone, Microstructure, and Surface Quality of TB8 Titanium Alloy Treated by Laser-Assisted Micromachining. *J. Mater. Eng. Perform.* **2022**, *31*, 2978–2990. [CrossRef]
5. Ullah, S.; Li, X.; Guo, G.; Rodríguez, A.R.; Li, D.; Du, J.; Cui, L.; Wei, L. Energy efficiency and cut-quality improvement during fiber laser cutting of aluminum alloy in the different hardened conditions. *Mater. Today Commun.* **2022**, *33*, 104236. [CrossRef]
6. Grešová, Z.; Ižol, P.; Vrabeľ, M.; Kaščák, Ľ.; Brindza, J.; Demko, M. Influence of Ball-End Milling Strategy on the Accuracy and Roughness of Free Form Surfaces. *Appl. Sci.* **2022**, *12*, 4421. [CrossRef]
7. Xu, Z.; Wang, Y. Study on cutting force and surface quality during slot milling of CFRP based on equivalent milling area. *Int. J. Adv. Manuf. Technol.* **2022**, *123*, 3377–3386. [CrossRef]
8. Vrabel, M.; Maňková, I.; Beňo, J. Monitoring and control of manufacturing process to assist the surface workpiece quality when drilling. *Proc. CIRP* **2016**, *41*, 735–739. [CrossRef]
9. Singh, S.; Singh, M.; Prakash, C.; Gupta, M.K.; Mia, M.; Singh, R. Optimization and reliability analysis to improve surface quality and mechanical characteristics of heat-treated fused filament fabricated parts. *Int. J. Adv. Manuf. Technol.* **2019**, *102*, 1521–1536. [CrossRef]
10. Peng, X.; Kong, L.; Fuh, J.Y.H.; Wang, H. A review of post-processing technologies in additive manufacturing. *J. Manuf. Mater. Process.* **2021**, *5*, 38. [CrossRef]
11. Miao, J.; Yu, D.; An, C.; Ye, F.; Yao, J. Investigation on the generation of the medium-frequency waviness error in flycutting based on 3D surface topography. *Int. J. Adv. Manuf. Technol.* **2017**, *90*, 667–675. [CrossRef]
12. Xu, J.; Zhang, X.; Zhu, F. Effects of machining parameters on surface morphology of porous bronze during monocrystalline diamond cutting. *Int. J. Mech. Sci.* **2022**, *234*, 107686. [CrossRef]
13. Žagar, S.; Soyama, H.; Grum, J.; Šturm, R. Surface integrity of heat treatable magnesium alloy AZ80A after cavitation peening. *J. Mater. Res. Technol.* **2022**, *17*, 2098–2107. [CrossRef]
14. Smith, S.; Melkote, S.N.; Lara-Curzio, E.; Watkins, T.R.; Allard, L.; Riester, L. Effect of surface integrity of hard turned AISI 52100 steel on fatigue performance. *Mater. Sci. Eng. A* **2007**, *459*, 337–346. [CrossRef]
15. Caruso, S.; Outeiro, J.; Umbrello, D.; Batista, A.C. Key Engineering Materials. In *Residual Stresses in Machining of AISI 52100 Steel under Dry and Cryogenic Conditions: A Brief Summary*; Trans Tech Publications: Zurich, Switzerland, 2014; pp. 1236–1242.
16. Matsumoto, Y.; Barash, M.; Liu, C. Effect of hardness on the surface integrity of AISI 4340 steel. *J. Eng. Ind.* **1986**, *108*, 169–175. [CrossRef]
17. Umer, U.; Mian, S.H.; Mohammed, M.K.; Abidi, M.H.; Moiduddin, K.; Kishawy, H. Self-Propelled Rotary Tools in Hard Turning: Analysis and Optimization via Finite Element Models. *Materials* **2022**, *15*, 8781. [CrossRef]

18. Savkovic, B.; Kovac, P.; Dudic, B.; Gregus, M.; Rodic, D.; Strbac, B.; Ducic, N. Comparative characteristics of ductile iron and austempered ductile iron modeled by neural network. *Materials* **2019**, *12*, 2864. [CrossRef]
19. Schill, F.; Michel, C.; Firus, A. Contactless Deformation Monitoring of Bridges with Spatio-Temporal Resolution: Profile Scanning and Microwave Interferometry. *Sensors* **2022**, *22*, 9562. [CrossRef]
20. Vorburger, T.V.; Rhee, H.-G.; Renegar, T.B.; Song, J.-F.; Zheng, A. Comparison of optical and stylus methods for measurement of surface texture. *Int. J. Adv. Manuf. Technol.* **2007**, *33*, 110–118. [CrossRef]
21. Mathiyazhagan, R.; SampathKumar, S.; Karthikeyan, P. Estimation of Surface Roughness on Milled Surface Using Capacitance Sensor Based Micro Gantry System through Single-Shot Approach. *Micromachines* **2022**, *13*, 1746. [CrossRef]
22. Taga, Ö.; Kiral, Z.; Yaman, K. Determination of cutting parameters in end milling operation based on the optical surface roughness measurement. *Int. J. Precis. Eng. Manuf.* **2016**, *17*, 579–589. [CrossRef]
23. Mauz, F.; Wigger, R.; Wahl, T.; Kuffa, M.; Wegener, K. Acoustic Roughness Measurement of Railway Tracks: Implementation of a Chord-Based Optical Measurement System on a Train. *Appl. Sci.* **2022**, *12*, 11988. [CrossRef]
24. Marsch, K.; Wujanz, D.; Fernandez-Steeger, T.M. On the usability of different optical measuring techniques for joint roughness evaluation. *Bull. Eng. Geol. Environ.* **2020**, *79*, 811–830. [CrossRef]
25. Fu, S.; Cheng, F.; Tjahjowidodo, T.; Zhou, Y.; Butler, D. A non-contact measuring system for in-situ surface characterization based on laser confocal microscopy. *Sensors* **2018**, *18*, 2657. [CrossRef] [PubMed]
26. Quinsat, Y.; Tournier, C. In situ non-contact measurements of surface roughness. *Precis. Eng.* **2012**, *36*, 97–103. [CrossRef]
27. Blateyron, F. Chromatic confocal microscopy. In *Optical Measurement of Surface Topography*; Springer: Berlin/Heidelberg, Germnay, 2011; pp. 71–106.
28. Rishikesan, V.; Samuel, G. Evaluation of surface profile parameters of a machined surface using confocal displacement sensor. *Procedia Mater. Sci.* **2014**, *5*, 1385–1391. [CrossRef]
29. Buajarern, J.; Kang, C.-S.; Kim, J.W. Characteristics of laser scanning confocal microscopes for surface texture measurements. *Surf. Topogr. Metrol. Prop.* **2013**, *2*, 014003. [CrossRef]
30. Wang, C.; Wang, G.; Shen, C. Analysis and Prediction of Grind-Hardening Surface Roughness Based on Response Surface Methodology-BP Neural Network. *Appl. Sci.* **2022**, *12*, 12680. [CrossRef]
31. Cui, Z.; Ni, J.; He, L.; Su, R.; Wu, C.; Xue, F.; Sun, J. Assessment of cutting performance and surface quality on turning pure polytetrafluoroethylene. *J. Mater. Res. Technol.* **2022**, *20*, 2990–2998. [CrossRef]
32. Cano-Salinas, L.; Sourd, X.; Moussaoui, K.; Le Roux, S.; Salem, M.; Hor, A.; Zitoune, R. Effect of process parameters of Plain Water Jet on the cleaning quality, surface and material integrity of Inconel 718 milled by Abrasive Water Jet. *Tribol. Int.* **2022**, *178*, 108094. [CrossRef]
33. Pahuja, R.; Ramulu, M.; Hashish, M. Surface quality and kerf width prediction in abrasive water jet machining of metal-composite stacks. *Compos. Part B Eng.* **2019**, *175*, 107134. [CrossRef]
34. Goyal, A.; Garimella, A.; Saini, P. Optimization of surface roughness by design of experiment techniques during wire EDM machining. *Mater. Today Proc.* **2021**, *47*, 3195–3197. [CrossRef]
35. Chahal, M.; Singh, V.; Garg, R. Optimum surface roughness evaluation of dies steel H-11 with CNC milling using RSM with desirability function. *Int. J. Syst. Assur. Eng. Manag.* **2017**, *8*, 432–444. [CrossRef]
36. Aziz, T.; Farid, A.; Haq, F.; Kiran, M.; Ullah, A.; Zhang, K.; Li, C.; Ghazanfar, S.; Sun, H.; Ullah, R. A review on the modification of cellulose and its applications. *Polymers* **2022**, *14*, 3206. [CrossRef]
37. Galus, S.; Arik Kibar, E.A.; Gniewosz, M.; Kraśniewska, K. Novel materials in the preparation of edible films and coatings—A review. *Coatings* **2020**, *10*, 674. [CrossRef]
38. Simchen, F.; Sieber, M.; Kopp, A.; Lampke, T. Introduction to plasma electrolytic oxidation—An overview of the process and applications. *Coatings* **2020**, *10*, 628. [CrossRef]